The Vela pulsar has a long history of γ-ray science. We present the finest time-resolved spectral study of the Vela pulsar to date.

Very Fine Time-Resolved Spectral Studies of the Vela Pulsar with the *Fermi* Large Area Telescope

T. J. Johnson[1,2,6], Ö. Çelik[2], M. Kerr[3], A. K. Harding[2], G. A. Caliandro[4,5] for the *Fermi* LAT Collaboration and Timing Consortium

The Vela pulsar is one of the most exciting γ-ray sources and has been at the forefront of high energy pulsar science since the detection of γ-ray pulsations at the radio period by SAS-2 in 1975. With the unprecedented angular resolution, effective area, field of view, and timing resolution, in the GeV band, of the Large Area Telescope (LAT) on the *Fermi Gamma-ray Space Telescope* the light curve of the Vela pulsar can be studied in greater detail than ever before. Using a timing solution derived solely from the LAT data, phase aligned with the radio emission, the spectrum of the Vela pulsar has been fit in intervals as small as 0.0016 in phase. Significant variation is seen in the cutoff energy and spectral index across the light curve, strongly supporting curvature radiation as the source of the high-energy γ-rays from the Vela pulsar.

Introduction:

The Vela pulsar has a long history of γ-ray observations dating back to the point source and pulsed detections with SAS-2 [1,2]. Phase-resolved spectral results followed using data from COS-B [3] and EGRET [4,5] suggesting significant variation of the spectrum across the pulse, with the hardest emission between the two main γ-ray peaks. The main instrument aboard *Fermi* is the Large Area Telescope (LAT) [6]. Soon after launch and commissioning[7] the LAT produced the highest resolution high-energy (HE), ≥0.1 GeV, light curve of the Vela pulsar to date, identified a third peak which moves with increasing energy, and ruled out low-altitude magnetospheric emission models [8].

Timing:

LAT data was used to construct a timing solution for the Vela pulsar with 63 μs residuals using techniques described in [9] and a plenary talk in this Symposium. The γ-ray timing solution* was phase aligned with data from the Parkes Radio Telescope [10].

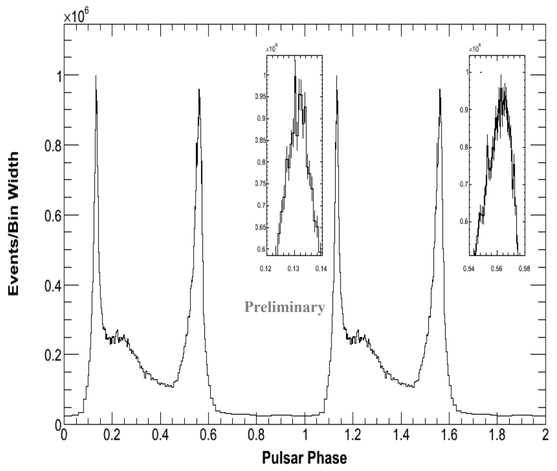

Figure 1: Folded light curve of the Vela pulsar for events with reconstructed energies ≥0.02 GeV and within max[1.3°,1.6°-3*log$_{10}$(E$_{Gev}$)] of the radio position, each bin has 750 counts.

LAT Data and Spectrum:

LAT event data from 4 August 2008 to 4 July 2009 and belonging to the "Diffuse" class [6], as defined under the P6_V3 instrument response functions, were selected within 15° of the radio position and having reconstructed energies [0.02,100] GeV. Further data selections are described in a forthcoming LAT paper [11]. Events were phase-folded using the fermi plug-in now provided with TEMPO2† [12]. The resulting γ-ray light curve is shown in Figure 1.

Events with energies ≥0.1 GeV were used for spectral analysis. The *Fermi* Science Tools‡ (STs) v9r15p2 were used to perform a binned maximum likelihood analysis [13,14] modeling nearby point sources; an extended source at the position of the Vela X pulsar wind nebula (PWN), see oral presentation by M. Lemoine-Goumard in parallel session 4 of this Symposium and [15]; and the v02 diffuse backgrounds, included with the *Fermi* STs. The phase-averaged spectrum (Figure 2) is best fit as an exponentially cutoff power law (Equation 1) with the b parameter <1, likely due to the superposition of many spectral components with b=1 and varying values of E_C and Γ through the pulse. This gives an integrated flux (0.1-100 GeV) of $1.07\pm0.01\pm0.03\times10^{-5}$ cm^{-2} s^{-1}, where the first errors are statistical and the second are systematic.

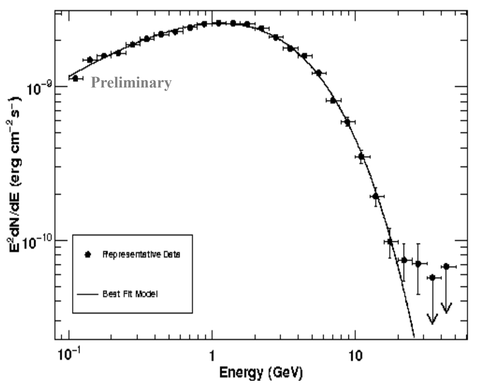

Figure 2: Phase-averaged γ-ray spectrum of the Vela pulsar. Best-fit model with b < 1. The representative data points are from likelihood fits to each energy range with the pulsar modeled as a power law.

$$\frac{dN}{dE} = N_0\left(\frac{E}{1\ \mathrm{GeV}}\right)^{-\Gamma} e^{-\left(\frac{E}{E_C}\right)^b} \qquad (1)$$

$N_0 = 4.13\pm0.15\pm1.16\times10^{-6}\ \mathrm{cm^{-2}\ s^{-1}\ GeV^{-1}}$
$\Gamma = 1.34 \pm 0.01^{+0.07}_{-0.03}$
$E_C = 1.11 \pm 0.07^{+0.88}_{-0.39}\ \mathrm{GeV}$
$b = 0.65 \pm 0.01^{+0.17}_{-0.09}$

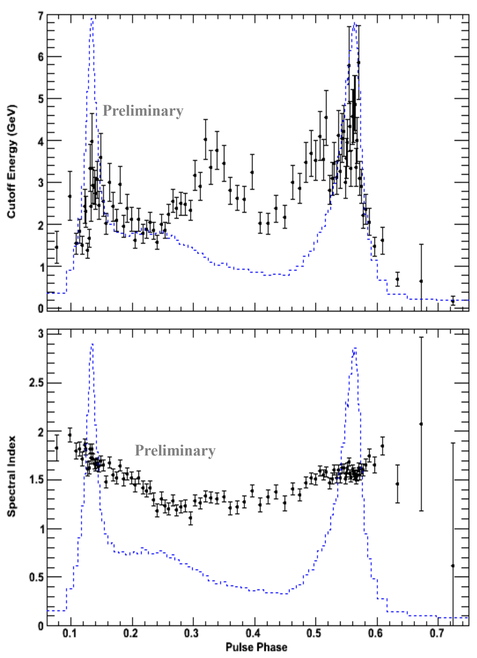

Phase-resolved Spectroscopy:

The light curve was divided into variable-width bins, 1500 events ≥0.1 GeV each, using the selection described in the caption of Figure 1. The smallest bin has a width of 0.0016 in phase (~142 μs). The spectrum of the Vela pulsar was fit assuming b=1 in each phase bin. Normalizations of the diffuse backgrounds and point sources within 5° of the pulsar were kept free. The observed trends in E_C and Γ are shown in Figure 3.

Significant variation is seen in both parameters, confirming that the hardest emission is between the two peaks. E_C rises sharply through the main peaks and between them as well, near the position of the observed third peak at higher energies. Phase-resolved analyses of EGRET data suggested a drastic change in Γ through the peaks; however, the LAT data does not confirm this, instead finding Γ to be very consistent with a constant value through both peaks, Figure 4.

Figure 3: (*Top*) Cutoff energy vs phase. (*Bottom*) Spectral index vs. phase. Errors are statistical only. Results are only shown for bins in which the pulsar was found above the background with a TS≥25.

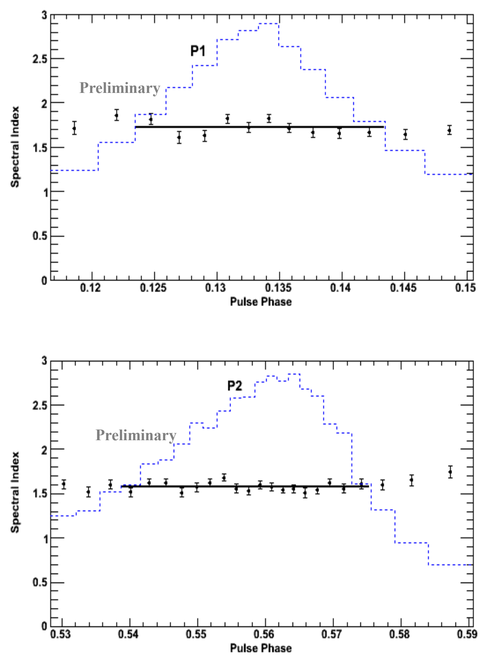

The Peaks:

To evaluate the significance of the features in Figure 3, the pulsar and surrounding region were simulated using the *Fermi* ST *gtobssim* and the built-in *PulsarSpectrum* [16]. The LAT-only timing parameters and spectral parameters from a phase-averaged fit with b=1 were input to the simulation. The simulation suggests that point-to-point variations of 0.6 GeV in E_C and 0.05 in Γ should be expected from the fitting technique. As such, point-to-point variations less than these values can not be considered significant.

To better evaluate the behavior of E_C in the peaks the fit was repeated with Γ fixed to the fit values in the two main peaks. The results for both peaks are shown in Figure 5. E_C rises fairly smoothly in both peaks with a maximum near the start of the trailing edges.

Figure 4: Spectral index vs. phase plots for the peaks, errors are statistical, black horizontal lines are best-fit constant values. (*Top*) Peak 1. (*Bottom*) Peak 2.

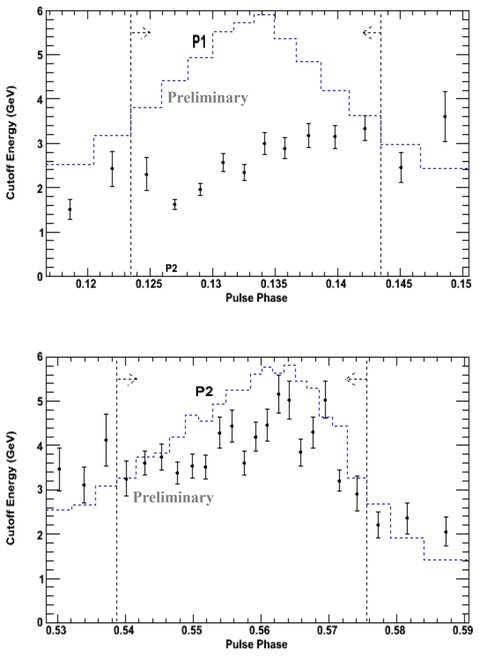

Figure 5: Cutoff energy vs. phase plots with the spectral index fixed through the peaks, errors are statistical, dashed lines and arrows show the peak definitions. (*Top*) Peak 1. (*Bottom*) Peak 2.

Discussion:

In outer-magnetospheric emission models, the HE γ-ray emission has been theorized to be curvature radiation from electrons (or positrons) accelerated along the B-field lines by the parallel component of the E-field ($E_\parallel$) [17,18]. In outer-magnetospheric emission models (e.g. slot gap (SG) [19], outer gap (OG) [20,21]) $E_\parallel$ depends on the B-field at the light cylinder and the gap width. These models give similar cutoff energies (Equation 2, in units of mc^2) ranging from 1 – 5 GeV, consistent with what is observed in Vela and other γ-ray pulsars.

$$E_{CR} = \frac{3}{2}\frac{\lambda}{\rho_c}\gamma_{CR}^3 = 0.32\ \lambda_c \left(\frac{E_\parallel}{e}\right)^{\frac{3}{4}} \rho_c^{\frac{1}{2}} \qquad (2)$$

The cutoff energy (E_{CR}) depends on the local field line radius of curvature (ρ_c). Emission across the pulse originates from different ranges of emission radii (OG [17,22] and two-pole caustic [23]), implying that the phase-resolved spectroscopy should map out the emission altitude. Large variations of ρ_c with phase are also expected and mapping the minimum ρ_c, using basic geometric models, can produce trends similar to those in Figure 3 (*Top*), but full radiation models will be needed to match all of the features. As the LAT continues to accumulate more events from Vela it will be possible to map the HE γ-ray emission regions in more detail and better understand the radiative processes involved.

Affiliations:
[1]Department of Physics, University of Maryland, College Park, MD 20742, USA
[2]NASA Goddard Space Flight Center, Greenbelt, MD 20771, USA
[3]Department of Physics, University of Washington, Seattle, WA 98195-1560
[4]Dipartimento di Fisica "M. Merlin" dell'Università e del Politecnico di Bari, I-70126 Bari, Italy
[5]Istituto Nazionale di Fisica Nucleare, Sezione di Bari, 70126 Bari, Italy
[6]Tyrel.J.Johnson@nasa.gov

References:
[1] Thompson, D. J., et al. 1974, ApJ, 190, L51
[2] Thomspon, D. J., et al. 1975, ApJ, 200, L79
[3] Grenier, I. A., Hermsen, W., Clear, J. 1988, A&A, 204, 117
[4] Kanbach, G., et al. 1994, A&A, 289, 855
[5] Fierro, J. M., et al. 1998, ApJ, 494, 734
[6] Atwood, W. B., et al. 2009, ApJ, 697, 1071
[7] Abdo, A. A., et al. 2009a, Astropart. Phys., *accepted* (arXiv:0904.2226)
[8] Abdo, A. A., et al. 2009b, ApJ, 696, 1084
[9] Ray, P. S., et al. 2009, *in preparation*
[10] Manchester, R. N. 2008, AIP Conf. Ser. 983, 584
[11] Abdo, A. A., et al. 2009c, *in preparation*
[12] Hobbs, G. B., Edwards, R. T., & Manchester, R. N. 2006, MNRAS, 369, 653
[13] Cash, W. 1979, ApJ, 228, 939
[14] Mattox, J. R. et al. 1996, ApJ, 461, 396
[15] Abdo, A. A., et al. 2009d, *in preparation*
[16] Razzano, M. et al. 2009, Astropart. Phys., 32, 1
[17] Romani, R. W. 1996, ApJ, 470, 469
[18] Hirotani, K. & Shibata, S. 1999, MNRAS, 308, 54
[19] Muslimov, A. G. & Harding, A. K. 2004, ApJ, 606, 1143
[20] Zhang, L., et al. 2004, ApJ, 604, 317
[21] Hirotani, K. 2008, Open Astronomy Journal, *submitted* (arXiv:0809.1283)
[22] Cheng, K. S., Ruderman, M. A., & Zhang, L. 2000, ApJ, 537, 964
[23] Dyks, J. & Rudak, B. 2003, ApJ, 598, 1201

*Timing solution will be made availabe on the FSSC website http://fermi.gsfc.nasa.gov/ssc/data/access/lat/ephems/
†http://tempo2.sourceforge.net/
‡http://fermi.gsfc.nasa.gov/ssc/data/analysis/scitools/overview.html